


 Cite this: *Lab Chip*, 2016, 16, 3548

# Transitioning from multi-phase to single-phase microfluidics for long-term culture and treatment of multicellular spheroids†

 Kay S. McMillan,<sup>a</sup> Marie Boyd<sup>b</sup> and Michele Zagnoni<sup>\*a</sup>

When compared to methodologies based on low adhesion or hanging drop plates, droplet microfluidics offers several advantages for the formation and culture of multicellular spheroids, such as the potential for higher throughput screening and the use of reduced cell numbers, whilst providing increased stability for plate handling. However, a drawback of the technology is its characteristic compartmentalisation which limits the nutrients available to cells within an emulsion and poses challenges to the exchange of the encapsulated solution, often resulting in short-term cell culture and/or viability issues. The aim of this study was to develop a multi-purpose microfluidic platform that combines the high-throughput characteristics of multi-phase flows with that of ease of perfusion typical of single-phase microfluidics. We developed a versatile system to upscale the formation and long-term culture of multicellular spheroids for testing anti-cancer treatments, creating an array of fluidically addressable, compact spheroids that could be cultured in either medium or within a gel scaffold. The work provides proof-of-concept results for using this system to test both chemo- and radio-therapeutic protocols using *in vitro* 3D cancer models.

 Received 12th July 2016,  
Accepted 27th July 2016

DOI: 10.1039/c6lc00884d

[www.rsc.org/loc](http://www.rsc.org/loc)

## 1. Introduction

Cancer continues to be a major problem worldwide, with a prediction that the number of new cases will reach over 20 million by 2030.<sup>1</sup> Although there has been an increase in the number of anticancer chemotherapies developed over the past decade, their success rate has been poor, with less than 10% of anticancer drugs progressing to clinical trials.<sup>2,3</sup> Furthermore, improvements are required in radiation therapy for certain types of cancer, such as glioblastoma, where treatment failure remains high.<sup>4</sup> To this end, more physiologically relevant preclinical cancer models than those based on cancer cell monolayers can lead to develop more efficacious therapies. Multicellular tumour spheroids are *in vitro* 3D cancer models which can mimic the heterogeneous cell composition and the microenvironmental features seen in *in vivo* tumours,<sup>3,5</sup> representing an ideal candidate model during drug discovery.<sup>6,7</sup> However, standard methods for the formation and study of multicellular tumour spheroids (*e.g.* spinner flask, hanging drop and low adhesion plates) are generally labour intensive and low-throughput.<sup>3</sup> Therefore, the develop-

ment of robust and automatable microfluidic technologies based on spheroid models has the potential to facilitate the adaptation of existing screening protocols and increase the data throughput when testing anticancer therapies.

In recent years, droplet microfluidics techniques<sup>8</sup> have been increasingly used for the formation and culture of multicellular spheroids and organoids.<sup>9–16</sup> These methods involve the encapsulation of cells or cell aggregates within an aqueous (or gel) droplet in an oil phase, with the aqueous–oil interface being biocompatible and presenting non-adhering characteristics.<sup>17,18</sup> In comparison to established methods, such as those based on spinner flasks or hanging drops, cell encapsulation in aqueous/gel-in-oil droplets prevents exposure of cells to shear stress<sup>19</sup> and provides a stable environment that is insensitive to mechanical perturbation, respectively.<sup>6</sup> Arguably, the greatest advantage that droplet microfluidics can offer is that of significantly increasing the throughput of information, where assays can be developed allowing the formation of up to 1000 spheroids per device.<sup>16</sup> However, a drawback of emulsion-based methods for cell culture is compartmentalisation, where each droplet acts as an environmentally isolated experiment, thus limiting the volume of nutrients available to the cells and concentrating build-up of waste products,<sup>11,12,20,21</sup> both of which have a detrimental effect on cell viability over time. Other limitations when working with emulsion techniques include the inability to directly perfuse the dispersed phase content and to prevent the partition of encapsulated substances (*i.e.* lipophilic drugs) into

<sup>a</sup> Centre for Microsystems and Photonics, Electronic and Electrical Engineering, University of Strathclyde, Glasgow, G1 1XW, UK.

E-mail: [michele.zagnoni@strath.ac.uk](mailto:michele.zagnoni@strath.ac.uk)

<sup>b</sup> Strathclyde Institute of Pharmacy and Biomedical Sciences, University of Strathclyde, Glasgow, G4 0RE, UK

† Electronic supplementary information (ESI) available. See DOI: 10.1039/c6lc00884d



the oil phase. Therefore, a microfluidic approach capable of overcoming these limitations would aid long-term cell culture after their encapsulation in emulsions and the development of multi-step anticancer treatment tests (*e.g.* repeated injection of drugs at specific time points after spheroid formation over weeks of culture).

It has been previously shown that biocompatible fluorosurfactants can be used for the formation and culture of spheroids within single and double emulsions.<sup>6,9</sup> This is obtained due to the polyethylglycol (PEG) head of the surfactant used, which creates a non-adherent water/oil interface, resulting in cancer cells aggregating within the emulsion to form compact spheroids. Additionally, we have shown that the ability to regulate the microenvironmental factors during spheroid culture within emulsions is a key aspect to ensure their viability and to control cell quiescence,<sup>6</sup> elements that affect spheroid response to radiotherapeutic investigation. Therefore, a microfluidic approach that integrates the compartmentalisation and high-throughput features of droplet microfluidics with the ease of perfusion of single-phase laminar flows would offer a universal microfluidic platform for screening multicellular spheroids.

The fluorosurfactants used in the previous studies are known to produce stable and long lasting emulsions when water or salt solutions were used as the dispersed phases.<sup>18</sup> However, it has been reported that molecules, such as bovine albumin serum (BSA), can destabilise the emulsion interface and increase their chance of coalescence.<sup>18</sup> This aspect could explain the need for microfluidic designs that keep emulsions from contacting each other when encapsulating cells.<sup>22</sup> Therefore, an approach that exploits induced interface instability to create controlled emulsion coalescence could provide a solution to the compartmentalization issues during cell culture with droplet microfluidics.

In this study, we present a microfluidic system that allows both chemotherapy and radiotherapy protocols to be investigated in an array of multicellular spheroids over weeks of culture. The procedure is based on the controllable coalescence of multiple emulsion interfaces after the initial spheroid formation, enabling injection of fresh media and drugs to be delivered at desired time points. The system was used to demonstrate culture of spheroids under various experimental conditions (*e.g.* with and without the use of 3D matrix scaffolds). Using a human glioma cell line (UVW),<sup>6</sup> we have characterised the growth rate of spheroids, their response to X-ray irradiation and to anticancer compounds, showing the wide range of applicability of the proposed microfluidic system to develop powerful screening assays.

## 2. Experimental

### 2.1. Device preparation

Microfluidic devices were fabricated using standard soft- and photo-lithography techniques as previously described.<sup>6</sup> Briefly, master templates were produced using SU8 photore-

sist (3000 series, MicroChem, US) onto a silicon wafer following the manufacturer's protocol, achieving a final resist thickness of 200  $\mu\text{m}$ . The resist was exposed through a photomask (JD Photo-Tools, UK) to UV light and was developed in Micro-Posit EC solvent (Rohm and Haas, US). Polydimethylsiloxane (PDMS) was poured onto the silicon master at a 10:1 ratio of base to curing agent, degassed in a vacuum desiccator chamber and cured at 80  $^{\circ}\text{C}$  for at least 2 hours. To prevent PDMS adhesion to the silicon master, the wafer's surface was silanised by vapour deposition of 1H,1H,2H,2H-perfluorooctyl-trichlorosilane (Sigma Aldrich, UK) for 1 hour. The PDMS devices were then peeled from the mould, cut to the desired size, and holes were punched using G21 needles to obtain inlet and outlet ports. PDMS devices were then cleaned and irreversibly bonded to glass microscope slides using oxygen plasma. Bonded devices were then treated with undiluted Aquapel (PPG Industries) to obtain fluorophilic microchannel surfaces.

### 2.2. Cell culture and spheroid formation

A human glioblastoma cell line (UVW) developed in house was utilised.<sup>23</sup> UVW cells were maintained in an atmosphere of 5%  $\text{CO}_2$  and incubated at 37  $^{\circ}\text{C}$ , in minimum essential medium (MEM), containing 10% (v/v) of foetal calf serum (FCS), L-glutamine (200  $\text{mmol l}^{-1}$ ), penicillin/streptomycin (100  $\text{U ml}^{-1}$ ) and Fungizone (2  $\mu\text{g ml}^{-1}$ ). Medium and additional supplements were purchased from Invitrogen, UK.

### 2.3. Microfluidic protocols

FC-40 (3 M) fluorinated oil with 2% wt block copolymer fluorosurfactants (designed by the Weitz Group at Harvard and supplied by RAN Biotechnologies, catalogue# 008-FluoroSurfactant, Beverly, MA, USA) was used as the continuous phase in all experiments. To better visualise the destabilisation of emulsion interfaces, an aqueous phase containing 100  $\mu\text{M}$  of calcein (Sigma Aldrich, UK) in either water or medium was used. For spheroid experiments, a cell suspension at a concentration of  $3 \times 10^6$  cells per ml in medium was used. Polytetrafluoroethylene (PTFE) tubing (Cole Parmer) was used to connect syringes to the inlet ports of the microfluidic device and syringe pumps (AL-1000, World Precision Instruments, Hertfordshire) were used to inject the phases. Two device structures were used: one to quantify emulsion coalescence in a large chamber (Fig. S1 in ESI†)<sup>24</sup> and another to carry out spheroid experiments (Fig. 2), based on a modified version of a previously reported design.<sup>25–27</sup> Medium in oil (M/O) droplets (with or without cells) were formed at a T-junction and then stored within the device. For spheroid culture, medium was refreshed every 2 days and devices were incubated after seeding at an atmosphere of 5%  $\text{CO}_2$  and at 37  $^{\circ}\text{C}$ . For spheroid withdrawal medium was dispensed through the outlet to displace spheroids from their traps.



#### 2.4. Alginate bead preparation

Sodium alginate (Sigma Aldrich, UK) was dissolved into medium at a concentration of 2% (w/v), heated to 50 °C for 2 hours and stored at 4 °C prior to use. The sodium alginate solution was filtered through a 0.2 µm filter to remove any particulate after storing it in a fridge. A cell suspension of  $3 \times 10^6$  cells per ml in the sodium alginate mixture was used as a dispersed phase. To carry out gelation of the alginate droplets, a 4% (w/v) solution of calcium chloride in medium was filtered through a 0.2 µm filter to remove any particulate and perfused through the device. After droplet gelation, the calcium chloride solution was replaced by medium which was subsequently refreshed every 2 days to replenish nutrients to the spheroids.

#### 2.5. Viability staining of spheroids

Spheroids were stained for cell viability using fluorescein diacetate (FDA) and propidium iodide (PI) (Sigma Aldrich, UK). The staining solution, containing 20 µg ml<sup>-1</sup> of PI and 8 µg ml<sup>-1</sup> of FDA, was loaded into a syringe and perfused through the device for approximately 20 minutes. Spheroids were incubated in the staining solution for approximately 15 minutes then washed with phosphate buffer saline (PBS) before imaging.

#### 2.6. Radiation treatment of spheroids

Spheroids were allowed to form and cultured in M/O droplets as previously described<sup>6</sup> and irradiated with a single dose of 8 Gy using a PXI X-Rad 225C X-irradiator, set to a dose rate equating to 2.2 Gy per min (RPS Services, Surrey, UK). Subsequently, both control and irradiated spheroids were cultured as previously described and their size monitored for up to 12 days.

#### 2.7. Dosimetry measurements

For calibration purposes, a UNIDOS® E universal dosimeter with a CC04 ionisation chamber (PTW, Germany) was used to measure the amount of radiation that was absorbed by a glass slide and a PDMS slab (~5 mm thick) respectively, as well as by a PDMS/glass microfluidic device.

#### 2.8. Drug treatment of spheroids

Cisplatin (Sigma Aldrich, UK) was dissolved in 0.9% sodium chloride solution to make a stock solution of 1 mM. Doxorubicin (Sigma Aldrich, UK) was dissolved in deionised water to make a stock solution of 5 mM. For treatment, the cisplatin stock solution was diluted to 50 µM with complete medium and the doxorubicin stock solution was diluted to 4 µM with complete medium. Spheroids were allowed to form and cultured in M/O droplets as previously described and perfused for 30 minutes with the desired anticancer compound. After 24 hours, the incubated drug solution was washed from the device and replaced by medium to replenish nutrient and create a favourable growth condition for the spheroids. Subsequently,

both control and cisplatin-treated or doxorubicin-treated spheroids were cultured for up to 12 or 14 days to assess treatment efficacy.

#### 2.9. Spheroid growth measurement

Spheroid growth was monitored over time by measuring the increase of their diameter after day 1 of culture (when compact spheroids were obtained) with brightfield microscopy, using a Zeiss inverted microscope (Axiovert A1) and a Labview controlled Dalsa Genie CMOS HM1024 camera. Spheroid dimensions were estimated using ImageJ by measuring the longest and shortest diameters (D1 and D2, respectively) to calculate their average diameter. The Mann Whitney test was used to evaluate the statistical difference between experiments (significant difference between groups obtained for  $p$  value  $\leq 0.05$ ).

### 3. Results and discussion

The device geometry and protocols developed in this work rely on the combination of a microfluidic passive channel network that enables M/O droplets, encapsulating a cell suspension, to be trapped within an array of sites and the controlled rupture of the emulsion interfaces once compact spheroids were formed within the array. Experiments were firstly conducted to determine the causes of emulsion coalescence. Subsequently, using the same device structure, microfluidic protocols were established for spheroid long-term culture using both complete medium (matrix-free condition) and calcium alginate gels (scaffold-supported condition) whilst performing periodic medium exchange. Finally, the system was validated for carrying out *in vitro* radiotherapeutic and chemotherapeutic assays using spheroids.

#### 3.1. Factors influencing emulsion coalescence

The fluorosurfactants used in this study are known to produce emulsions with robust,<sup>18</sup> long-lasting<sup>28</sup> and biocompatible oil/water interfaces, thus enabling favourable conditions for the culture of cells, organisms<sup>20</sup> and multicellular spheroids.<sup>6</sup> However, when emulsions containing cell medium were incubated in close contact with each other and in static conditions, we observed undesired and increasing emulsion coalescence over a period of time ranging from tens of minutes to a few hours, a condition that never occurred when encapsulating deionised water solutions. Therefore, we investigated the factors that compromised emulsion stability by testing emulsion coalescence when using various aqueous phases that are typically required for the culture of mammalian cells. In addition, these experiments were also carried out investigating the effects on coalescence due to temperature variation and mechanical shocks, practical factors involved in the long-term culture of cells and when handling microfluidic devices from cell incubators to microscope stages or plate readers. The aqueous phases included deionised water, PBS, MEM without additives, MEM with



individual additives and the complete cell medium used for cell culture of UVW cells (*i.e.* containing growth factors, anti-fungals, antibiotics, *etc.*).

To carry out this investigation, aqueous droplets in oil were formed and stored within a microfluidic chamber (~1300 aqueous droplets per chamber) that allowed for emulsion interfaces to be in close contact with each other (Fig. S1 in ESI†). The number of non-coalesced emulsions in the chamber upon initial loading was compared to the number of non-coalesced emulsions after 30 minutes under three conditions: while stationary, within an incubator at 37 °C, or after a 'mild' mechanical shock produced by placing the device on a microscope stage holder. This analysis provided the resulting percentage of emulsion coalescence for each case (Fig. 1) which was calculated as follows:

$$\%_{\text{Coalescence}} = \frac{N_{\text{Droplets}}(t=0) - N_{\text{Droplets}}(t=x)}{N_{\text{Droplets}}(t=0)} \times 100, \quad (1)$$

where  $N_{\text{Droplets}}(t=0)$  equals the number of droplets at the start of the experiment and  $N_{\text{Droplets}}(t=x)$  equals the number of droplets after a certain period of time. As expected, and in agreement with the literature, when using deionised water, PBS or MEM without supplements (1–3 in Fig. 1A), no coalescence was observed except for the case of incubating droplets at 37 °C. In contrast, when medium was used in combination with any of the supplements (4–9 in Fig. 1A), droplet coalescence increased significantly even when the device was kept stationary and at ambient temperature. In these conditions, a mild physical shock (*i.e.* produced by placing the device on a microscope holder) was observed to increase the chance of coalescence by twice as much with respect to its stationary state. As expected, storing the device inside a cell incubator showed a progressive increase in coalescence from deionised water to PBS and from MEM to full medium. Above all, additives typically used for cell culture, such as FBS, Fungizone and penicillin/streptomycin, strongly enhanced the instability of the emulsion interface in comparison to minimum essential medium alone. As previously described for emulsions made using the same fluorosurfactants, additive molecules within the encapsulated phase, such as bovine serum albumin (BSA),<sup>18</sup> can interact with the surfactant monolayer at the emulsion interface, resulting in the displacement of the surfactants and leading to emulsion coalescence. Relevant to our study, one of the components of FBS is albumin and it can be assumed that this molecule, in combination with other supplements, could be responsible for the increased emulsion instability observed. However, due to the complexity and variety of additives in full cell medium, further investigation needs to be carried out to identify other potential molecular causes related to coalescence.

### 3.2. Device operation principle: from emulsions to single phase microfluidics

The analysis presented in the previous section highlighted how molecules typically present in cell culture medium can

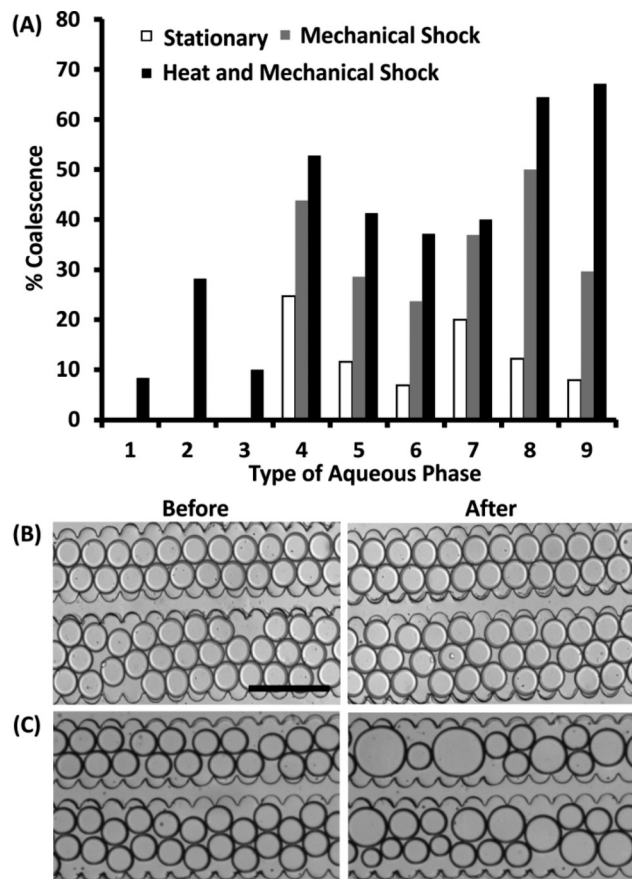
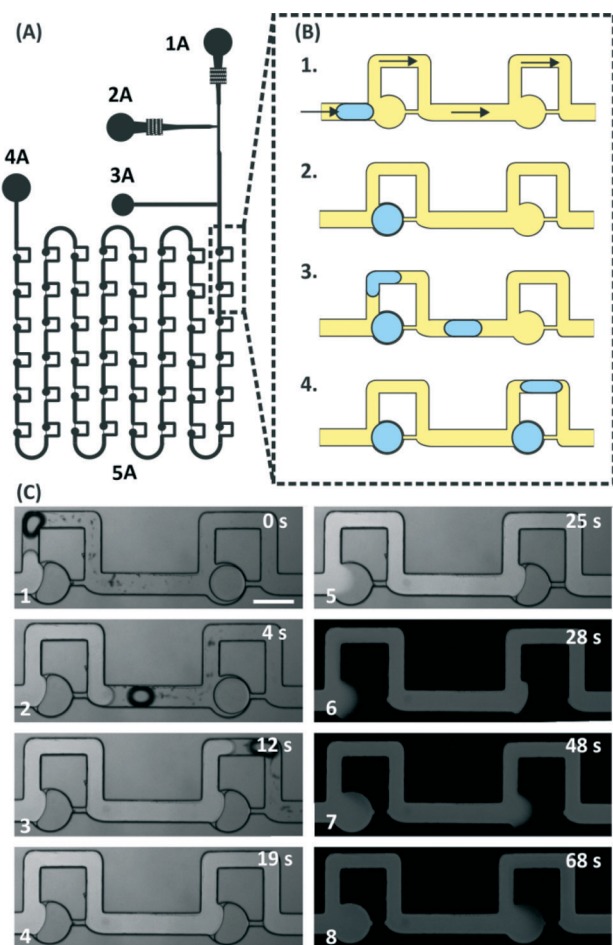


Fig. 1 Effect of the aqueous phase composition on coalescence of contacting emulsions. (A) Bar chart showing the percentage of coalesced emulsions for different aqueous phases in varied experimental conditions. An initial number of approximately 1000 emulsions ( $N_{\text{Droplet}}(t=0) = 1000$  in eqn (1)) were considered for each case (1 trial per case is shown). After droplet formation, emulsions were stored in a microfluidic chamber: (white) devices were kept stationary on a microscope stage for 30 min; (grey) devices were manually placed on a microscope stage producing a mild mechanical shock; (black) devices were transferred from a cell incubator at 37 °C to the microscope stage after 30 min. The  $\%_{\text{Coalescence}}$  value was calculated using eqn (1). Representative images of coalescence of droplet in oil-surfactants within a microfluidic chamber using deionised water (B) and complete medium (C) before and after placing the device on a microscope. 1 is deionised water; 2 is PBS; 3 is MEM; 4 is MEM with FBS; 5 is MEM with Fungizone; 6 is MEM with Pen/Strep; 7 is MEM with FBS and Pen/Strep; 8 is MEM with FBS and Fungizone and 9 is MEM with all of the supplements for UVW cell culture. The scale bar is 350  $\mu\text{m}$ .

facilitate emulsion coalescence. Here, we exploit this aspect to our advantage. We present a two steps procedure whereby droplet microfluidics protocols were first used to encapsulate cells within emulsions and allowed their transformation into multicellular spheroids in compartmentalized growth sites in parallel. Subsequently, within the same microfluidic structure, perfusion of complete medium replaced the continuous oil phase and resulted in the controlled rupture of the emulsion interfaces, thus enabling subsequent medium exchange, guaranteeing long term culture and the delivery of chemicals to the pre-formed spheroids at the desired time points.





**Fig. 2** Microfluidic protocol for emulsion production, storage and interface disruption. (A) Layout of the microfluidic device: aqueous phase-in-oil plugs are generated at a T-junction; 1A is the oil phase inlet; 2A is the aqueous phase inlet; 3A is the bypass channel outlet; 4A is the outlet and 5A is the chamber array. (B) Schematic diagram showing the plug trapping mechanism: a plug approaches an empty storing chamber and remains trapped within it (1 and 2); subsequent plugs bypass the occupied round chamber and enter in the next available trap (3 and 4) (Movie S1†). (C) Time-lapse of brightfield & fluorescent images (1 to 5) and fluorescent images (6 to 8) of a long plug containing medium with calcein interacting with emulsion interfaces and eventually leading to interface rupture. Images 1 to 4 show the long plug entering the serial array and coming into contact with the droplets in the traps without initial coalescence. Images 5 to 8 show the sequential rupture of the interface between the stored droplets and plug. Calcein is then observed to diffuse inside the stored droplet following emulsion interface rupture (Movie S2†). The scale bar is 400  $\mu\text{m}$ .

For this, a microfluidic design was developed based on the work by Boukellal *et al.*<sup>25</sup> and Vanapalli *et al.*<sup>26,27,29</sup> The microfluidic channel network consisted of a serial array of traps allowing for the sequential storage of M/O droplets (Fig. 2A). When a plug approached an empty trapping site, it followed the path with the smallest fluidic resistance and entered a round chamber within which its surface tension energy was minimised, with the emulsion changing its shape from an oblong plug to a round droplet (Fig. 2B 1–2). A subsequent plug would bypass the trapped droplet without coa-

lescence and slot in the next available empty round chamber (Fig. 2B 3–4) until all the trapping sites were occupied (Movie S1†). At this point, only the continuous phase was flown through the device channels to remove any non-trapped droplet and exited the device both from the array and the bypass channel outlets (3A and 4A in Fig. 1). In this condition, tubing was detached from the device with the emulsions remaining ‘locked’ into the round chambers, enabling spheroid incubation for as long as required.

To induce rupture of the emulsion interfaces, a solution of full medium (containing molecules that could destabilise the emulsion interface as previously discussed) was injected into the device after 24 hours. This formed a long plug that pushed the oil left in the microchannel towards the outlets without displacing the trapped droplets (Fig. 2C 1–4). Subsequently, coalescence of the trapped droplets with the long plug was observed within minutes (Fig. 2C 5–8 and Movie S2†). As a control experiment, when water was used as the aqueous phase, no coalescence of the plug with the trapped droplets occurred (not shown).

In contrast to previous reports,<sup>27,30</sup> by following this protocol, emulsion coalescence occurred without the need to alter the surfactant concentration in the oil phase and with a relatively simple procedure that did not require the use of active PDMS valves or electrocoalescence strategies.<sup>31,32</sup> Whilst for organisms such as *C. Elegans* low concentration of surfactants (0.001% w/v) are typically tolerated,<sup>30</sup> when using mammalian cell suspensions the biocompatibility guaranteed by the PEG-fluorocarbon surfactants (2% w/v) is essential for long term culture and to provide a non-adherent interface which is required to induce cellular aggregation.<sup>6</sup>

### 3.3. Formation and culture of multicellular spheroids

We have previously demonstrated how emulsion technologies can be exploited to control the level of proliferation and quiescence of multicellular spheroids.<sup>6</sup> However, the major limitation to scaling up the techniques developed was the need for accessing and exchanging the emulsion inner phase, procedures that were carried out manually. In this work, following the protocol detailed in section 3.2, we demonstrate proof-of-concept of *in vitro* chemotherapy and radiotherapy assays within a single, scalable and automatable microfluidic platform, enabling direct access to the cultured spheroid micro-environment to be obtained *via* microfluidic perfusion.

Here, spheroids were formed in plugs containing a suspension of glioma cells and these were trapped within the storage array. In brief, a cell suspension incubated in a resting droplet sedimented at the bottom of the droplet on the biocompatible PEG layer at the medium/oil interface. Due to the non-adherent nature of the PEG head of the fluorosurfactants, cells tended to aggregate into a compact spheroid structure.<sup>6</sup> Droplet trapping efficiency was 100%, with each droplet encapsulating between 60 and 160 cells for the cell concentration used (Fig. 3). This variation in cell number within droplets is due to the fact that particle



encapsulation in emulsions follows a Poisson distribution.<sup>33</sup> Additionally, we sometimes observed a fluctuation in the flow due to cell clustering that influenced the number of cell encapsulated per M/O droplet. After trapping, droplets containing cells were incubated for approximately 24 hours at 5% CO<sub>2</sub> and at 37 °C, allowing for the formation of compact cell aggregates, as previously described.<sup>6</sup> During this step, the use of PEG-fluorocarbon surfactants was essential to guarantee a non-adherent substrate, thus inducing cell aggregation. Although a slight shrinkage of the M/O droplets was observed over this time (which can be compensated for by increasing the humidity level during incubation), due to medium evaporation, the emulsions did not displace from the traps and no detrimental effects were produced to spheroid viability.

After 1 day of culture, compact spheroids were obtained, ranging from 40 to 150 μm in diameter depending on the initial cell number within the M/O droplet (Movie S3<sup>†</sup>). Overall, spheroid size variation within a device can be advantageous when performing screening assays as, due to the proportion of quiescent to proliferative cells in a spheroid, different responses to treatment can be observed.<sup>6</sup> After 24 hours, a long plug of medium was created in the device to coalesce the interface of the emulsions containing spheroids, with spheroids being occasionally displaced from the trapping sites if their size was <40 μm. Subsequently, the device was perfused every 2 days with fresh medium for 30 minutes (at 0.5 μL min<sup>-1</sup>) and the growth of spheroids was monitored by brightfield microscopy. As shown in Fig. 3, spheroids

remained compact and did not adhere to the device substrate for a period of 17 days (max time point tested in this work). Therefore, this suggests that a non-adherent PEG-layer is maintained in the trapping sites even after interface rupture and oil removal. Spheroids grew over time, suggesting that the medium perfusion protocol was adequate to supply cells with the required nutrition for proliferation, as well as to remove waste products. The viability of spheroids was confirmed by carrying out live/dead staining with FDA and PI, with no dead cells observed after 17 days of culture for the control experiments. These findings demonstrate that spheroid long-term culture can be robustly achieved using this approach.

For the cell line used, only viability staining was conducted as the UVW glioma cell line does not change cell characteristics according to treatment. However, if other cell types were used and specific biomarkers were released, any appropriate immunoassay could be carried out and/or analysis of the retrieved medium (10–15 μL) could be conducted. Additionally, we also developed a procedure to retrieve the spheroids from the microfluidic device after formation. This was obtained by injecting medium from the outlet (4A in Fig. 2) which displaced the spheroids slowly from their trapping sites (Fig. S2<sup>†</sup>), leading them into the main serpentine. Spheroids ultimately exited the device from the auxiliary outlet (3A in Fig. 2) for off-chip post-processing if required (*e.g.* spheroid sectioning or flow cytometry analysis). The viability of spheroids extracted from the device was confirmed by carrying out live/dead staining with FDA and PI from control

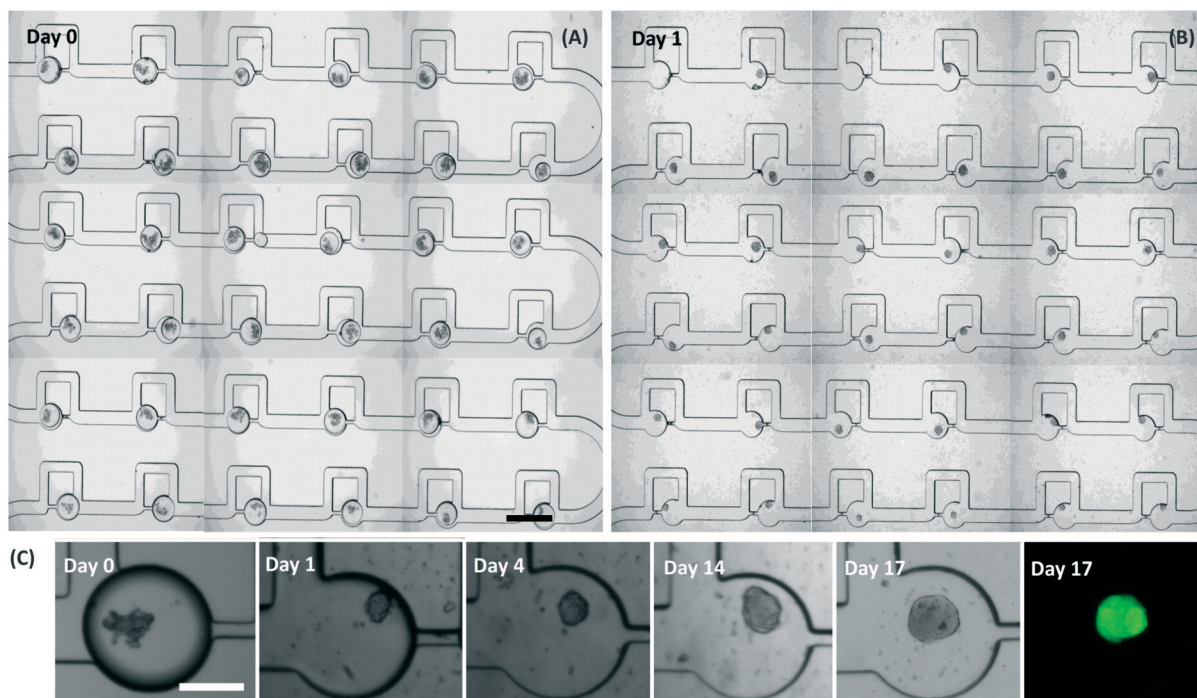


**Fig. 3** Formation and culture of multicellular glioma spheroids. (A) Stacked brightfield images of cell suspensions encapsulated in aqueous droplets trapped within the array on day 0. For clarity of image, 30 trapping sites are shown out of the 48 available. (B) Same field of view after interface rupture on day 1 showing formation of spheroids. (C) Representative time-lapse images of spheroid formation and growth over 17 days, at which the spheroids were stained for viability with FDA and PI. The scale bar for (A) and (B) is 400 μm and for (C) is 200 μm.



experiments, showing that the procedure had no detrimental effect to the integrity of the multicellular structure.

Other multiphase approaches in the literature have included the use of microfluidic double emulsions for spheroid culture. However, a progressive reduction in cell viability of cells was reported over time and was attributed to the fact that growth factors were unable to diffuse across the oil layer.<sup>9,34</sup> In addition, with respect to the present study, the formation of double emulsions adds complexity to the droplet formation process (mainly due to the need for hydrophilic/hydrophobic patterns) with respect to single emulsions.

Finally, the developed microfluidic protocols were tested to provide proof-of-concept results for scalable chemo- and radio-therapeutic assays.

### 3.4. Spheroid response to irradiation and drug treatment

Prior to cell-based experiments, dosimetry measurements were carried out to determine if any radiation was absorbed by the device materials, resulting in approximately 8% of the radiation intensity to be absorbed by the PDMS layer (~5 mm thick).

Spheroids were treated with a single dose of 8 Gy X-ray irradiation on day 7 of culture and their size monitored in comparison to a control experiment (unirradiated spheroids). A value of 8 Gy irradiation was chosen as previous experiments had shown that UVW glioma spheroids are highly radioresistant.<sup>6</sup> A significant reduction ( $p < 0.001$ ) in spheroid diameter was observed in comparison to the control experiment on day 12 of culture (Fig. 4A), which was confirmed by live/dead staining (Fig. 4B).

Alternatively, following the protocol described in section 3.3, spheroids were formed and a solution of either cisplatin or doxorubicin was perfused through the device on day 7 of culture. The spheroids were then left to incubate in the presence of the drug for 24 hours. Subsequently, medium was perfused through the device to wash out the drug solution. A significant reduction ( $p < 0.01$ ) in spheroid diameter was observed in comparison to the control (no drug) 7 days after treatment for cisplatin and 5 days after treatment for doxorubicin (Fig. 5A). On day 14 for cisplatin and day 12 for doxorubicin, a significant amount of cells had disaggregated from the spheroids (Fig. 5B and C) and their viability assessed using live dead staining. As for irradiated spheroids, if their size was considerably reduced, medium exchange could lead to spheroid displacement from their site of culture. Our previous study<sup>6</sup> has shown that radiation treatment and relapse mechanisms are dependent on the number of quiescent and proliferative cells in a spheroid. This microfluidic protocol could be used to scale-up the investigation of such effects using combination therapy and implementing protocols based on multiple steps of drug delivery. The device structure used in our experiments hosted 48 spheroids (Fig. 2), allowing for statistical information to be extracted from a single device per treatment and for differently sized spheroids.

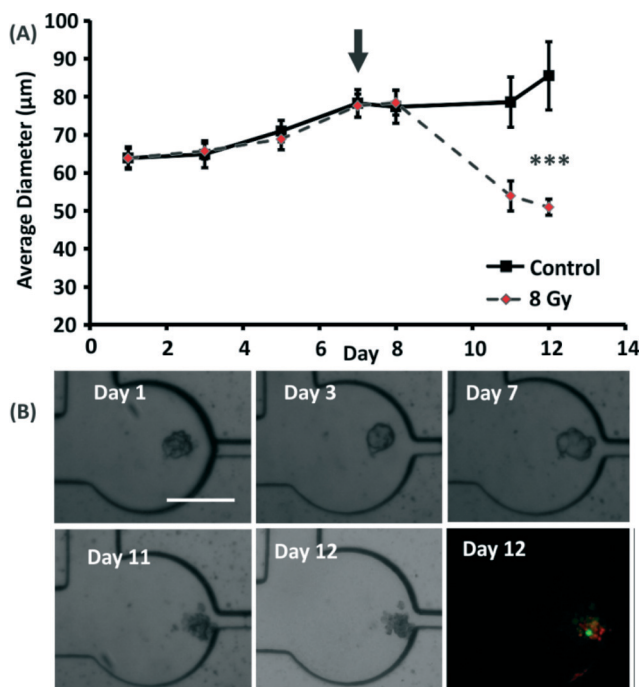


Fig. 4 Radiation treatment of glioma spheroids. (A) The growth curve shows the average spheroid diameter ( $\mu\text{m}$ ) over days of culture in the microfluidics for both control (untreated spheroids – continuous line) and radiation experiments (spheroid treated with 8 Gy on day 7 – as indicated by the arrow – dashed line) with the error bars representing the standard error of the mean ( $n = 23$ ). (B) Representative time-lapse images of the radiation experiment with live/dead stain on day 12. The scale bar is  $200 \mu\text{m}$ . \*\*\* represents a  $p$  value  $\leq 0.001$ . The reduction in spheroid size in combination with viability staining is used as an indicator of spheroid health and efficacy of the treatment.

However, the channel design is scalable and the protocol developed can be easily adapted according to the size of the substrate used and the readout instrumentation. In the future, in order to increase the number of drug concentrations tested simultaneously, multiple devices with  $N$  spheroids could be connected in parallel by linking an inlet from each device to an outlet of a microfluidic gradient generator. This would enable  $N$  repeats for several drug concentrations to be performed on the same substrate, achieving similar outcomes as to those obtained in 384 well plates,<sup>35</sup> with no requirements for expensive robotic dispensing instrumentation, as well as allowing for gel scaffolds to be used for cell culture.

### 3.5. Spheroid formation in alginate beads

Recurrently, alginate beads or microcapsules have been used in spheroid-based microfluidic studies,<sup>12,15,18</sup> rather than aqueous droplets, due to the ease of perfusing solutions through the gel porous structure and with the idea of providing a 3D scaffold environment as a beneficial support for cell culture.<sup>11,36</sup> Therefore, the developed microfluidic protocol was also tested to determine its suitability for carrying out spheroid culture within alginate beads.



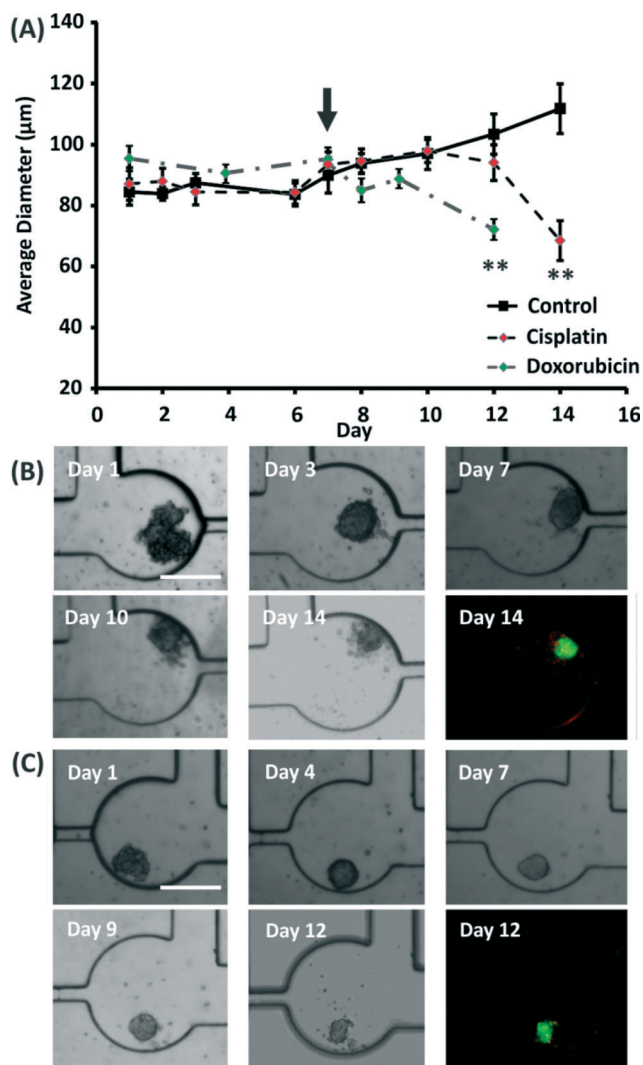


**Fig. 5** Drug treatment of spheroids. The growth curve (A) shows the average spheroid diameter over 12 to 14 days for control (untreated spheroids – continuous line), cisplatin (spheroids treated with 50  $\mu\text{M}$  – as – dashed black line) and doxorubicin (spheroids treated with 4  $\mu\text{M}$  – dashed-dot grey line) experiments. The arrow indicates the day of treatment for both drugs (day 7) applied for 24 hours. The error bars represent the standard error of the mean ( $n = 18$ ). Representative time-lapse images of spheroids (B) treated with cisplatin and (C) treated with doxorubicin with FDA and PI staining performed on day 14 or 12 respectively. The scale bar is 200  $\mu\text{m}$ . \*\* represents a  $p$  value of  $\leq 0.01$ . The reduction in spheroid size in combination with viability staining is used as an indicator of spheroid health and the efficacy of the treatment.

To achieve alginate gelation, divalent cations such as calcium ions are required to cross link with the carboxylic groups of the G block monomers which make up part of the alginate polysaccharide.<sup>37</sup> Alginate droplets containing cells were formed and used as described in section 3.3. Once the droplets were trapped within the array in the round chambers, a calcium chloride solution was flown through the channels to promote alginate gelation by diffusion through the emulsion interface (Fig. 6C–E). Occasionally, a reduction in the alginate bead size was observed over time. This behav-

our has been previously reported and is thought to be due to the release of  $\text{Ca}^{2+}$  into the medium.<sup>36</sup>

In contrast to spheroids formed within aqueous droplets (Fig. 6A and B), the cells encapsulated in alginate beads aggregated at a slower rate (3–4 days passed before spheroid formation), initially forming less smooth and compact spheroids, with some cells remaining separated from the main spheroid body throughout the culture. Similar characteristics

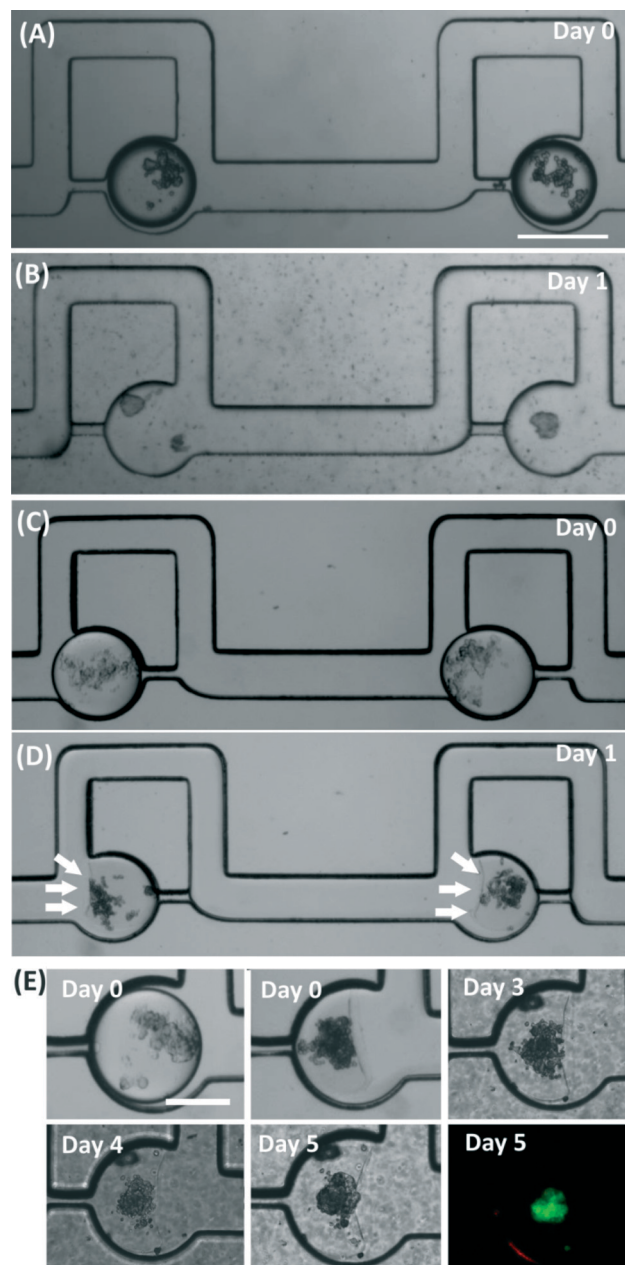


**Fig. 6** Formation of spheroids within alginate beads. Brightfield images showing cells encapsulated in medium with alginate (A and C) on day 0 and after interface rupture using medium with (B) and without (D) calcium chloride. White arrows in (D) points to the alginate interface formed after perfusion of calcium chloride. (E) Representative time-lapse images of spheroids formed within alginate beads and stained with FDA and PI on day 5. The scale bars for A–D is 400  $\mu\text{m}$  and for E is 200  $\mu\text{m}$ .





for cell aggregation and spheroid formation have been previously shown.<sup>10,11</sup> Furthermore, within alginate droplets which were not exposed to calcium chloride, the cells aggregated much faster, with times comparable to those when using aqueous droplets. This reinforces the idea that cell aggregation is delayed when cells are embedded in a more viscous gel environment.

## 4. Conclusion

In this work, we have developed a new microfluidic protocol that harnesses the advantages of the compartmentalisation properties of droplet microfluidics to create multicellular spheroids and those of controllable perfusion typical of single-phase microfluidics. The proposed methodology is scalable and enables the transition from multi-phase to single-phase flows, thus allowing long-term cell culture, drug perfusion and is amenable to cell culture applications that require the use of gel scaffolds. We have obtained proof-of-concept data demonstrating spheroid response to radiation and chemotherapy agents and have shown that the protocol can be used with both aqueous and alginate beads (scaffold-supported cell culture), allowing for user-defined culture conditions to be implemented. In the future, this system has the potential to be further scaled-up for drug concentration tests and used for *in vitro* radiotherapy and chemotherapeutic combination treatments to identify potential radiosensitising agents for radioresistant tumours.

## Acknowledgements

We would like to thank the Engineering and Physical Sciences Research Council (EP/K503174/1) and the University of Strathclyde for financial support. We thank Dr Annette Sorensen for help with calibration during radiation experiments.

## References

- 1 F. Bray, A. Jemal, N. Grey, J. Ferlay and D. Forman, Global cancer transitions according to the Human Development Index (2008-2030): a population-based study, *Lancet Oncol.*, 2012, **13**, 790–801.
- 2 W. N. Hait, Anticancer drug development: the grand challenges, *Nat. Rev. Drug Discovery*, 2010, **9**, 253–254.
- 3 S. Breslin and L. O'Driscoll, Three-dimensional cell culture: the missing link in drug discovery, *Drug Discovery Today*, 2013, **18**, 240–249.
- 4 A. C. Begg, F. a. Stewart and C. Vens, Strategies to improve radiotherapy with targeted drugs, *Nat. Rev. Cancer*, 2011, **11**, 239–253.
- 5 J. Kahn, P. J. Tofilon and K. Camphausen, Preclinical models in radiation oncology, *Radiat. Oncol.*, 2012, **7**, 223.
- 6 K. S. McMillan, A. G. McCluskey, A. Sorensen, M. Boyd and M. Zagnoni, Emulsion technologies for multicellular tumour spheroid radiation assays, *Analyst*, 2016, **141**, 100–110.
- 7 O. Trédan, C. M. Galmarini, K. Patel and I. F. Tannock, Drug resistance and the solid tumor microenvironment, *J. Natl. Cancer Inst.*, 2007, **99**, 1441–1454.
- 8 A. B. Theberge, *et al.*, Microdroplets in microfluidics: an evolving platform for discoveries in chemistry and biology, *Angew. Chem., Int. Ed.*, 2010, **49**, 5846–5868.
- 9 H. F. Chan, *et al.*, Rapid formation of multicellular spheroids in double-emulsion droplets with controllable microenvironment, *Sci. Rep.*, 2013, **3**, 3462.
- 10 S. Yoon, J. A. Kim, S. H. Lee, M. Kim and T. H. Park, Droplet-based microfluidic system to form and separate multicellular spheroids using magnetic nanoparticles, *Lab Chip*, 2013, **13**, 1522–1528.
- 11 L. Yu, M. C. W. Chen and K. C. Cheung, Droplet-based microfluidic system for multicellular tumor spheroid formation and anticancer drug testing, *Lab Chip*, 2010, **10**, 2424–2432.
- 12 C. Kim, *et al.*, Generation of core-shell microcapsules with three-dimensional focusing device for efficient formation of cell spheroid, *Lab Chip*, 2011, **11**, 246–252.
- 13 Y. Wang and J. Wang, Mixed hydrogel bead-based tumor spheroid formation and anticancer drug testing, *Analyst*, 2014, **139**, 2449–2458.
- 14 K. Alessandri, *et al.*, Cellular capsules as a tool for multicellular spheroid production and for investigating the mechanics of tumor progression *in vitro*, *Proc. Natl. Acad. Sci. U. S. A.*, 2013, **110**, 14843–14848.
- 15 S. Sugaya, M. Yamada and M. Seki, Manipulation of cells and cell spheroids using collagen hydrogel microbeads prepared by microfluidic devices, *2012 Int. Symp. Micro-NanoMechatronics Hum. Sci.*, 2012, pp. 435–438, DOI: 10.1109/MHS.2012.6492486.
- 16 P. Sabhachandani, *et al.*, Generation and Functional Assessment of 3D Multicellular Spheroids in Droplet Based Microfluidics Platform, *Lab Chip*, 2015, **16**, 497–505.
- 17 D. J. Holt, R. J. Payne and C. Abell, Synthesis of novel fluororous surfactants for microdroplet stabilisation in fluororous oil streams, *J. Fluorine Chem.*, 2010, **131**, 398–407.
- 18 C. Holtze, *et al.*, Biocompatible surfactants for water-in-fluorocarbon emulsions, *Lab Chip*, 2008, **8**, 1632–1639.
- 19 R.-Z. Lin and H.-Y. Chang, Recent advances in three-dimensional multicellular spheroid culture for biomedical research, *Biotechnol. J.*, 2008, **3**, 1172–1184.
- 20 J. Clausell-Tormos, *et al.*, Droplet-based microfluidic platforms for the encapsulation and screening of Mammalian cells and multicellular organisms, *Chem. Biol.*, 2008, **15**, 427–437.
- 21 F. Chen, *et al.*, Chemical transfection of cells in picoliter aqueous droplets in fluorocarbon oil, *Anal. Chem.*, 2011, **83**, 8816–8820.
- 22 C. H. J. Schmitz, A. C. Rowat, S. Köster and D. a. Weitz, Dropspots: a picoliter array in a microfluidic device, *Lab Chip*, 2009, **9**, 44–49.
- 23 M. Boyd, A. Livingstone, L. E. Wilson, E. M. Marshall, A. G. McCluskey, R. J. Mairs and T. E. Wheldon, Dose–response relationship for radiation-induced mutations at micro- and



- minisatellite loci in human somatic cells in culture, *Int. J. Radiat. Biol.*, 2000, 76, 169–176.
- 24 C. Martino, *et al.*, Intracellular protein determination using droplet-based immunoassays, *Anal. Chem.*, 2011, 83, 5361–5368.
- 25 H. Boukellal, S. Selimović, Y. Jia, G. Cristobal and S. Fraden, Simple, robust storage of drops and fluids in a microfluidic device, *Lab Chip*, 2008, 9, 331–338.
- 26 S. S. Bithi and S. a. Vanapalli, Behavior of a train of droplets in a fluidic network with hydrodynamic traps, *Biomicrofluidics*, 2010, 4, 44110.
- 27 M. Sun, S. S. Bithi and S. a. Vanapalli, Microfluidic static droplet arrays with tuneable gradients in material composition, *Lab Chip*, 2011, 11, 3949–3952.
- 28 J.-C. Baret, *et al.*, Fluorescence-activated droplet sorting (FADS): efficient microfluidic cell sorting based on enzymatic activity, *Lab Chip*, 2009, 9, 1850–1858.
- 29 S. S. Bithi, W. S. Wang, M. Sun, J. Blawdziewicz and S. a. Vanapalli, Coalescing drops in microfluidic parking networks: A multifunctional platform for drop-based microfluidics, *Biomicrofluidics*, 2014, 8, 034118.
- 30 H. Wen, Y. Yu, G. Zhu, L. Jiang and J. Qin, A droplet microchip with substance exchange capability for the developmental study of *C. elegans*, *Lab Chip*, 2015, 15, 1905–1911.
- 31 M. Zagnoni, G. Le Lain and J. M. Cooper, Electrocoalescence mechanisms of microdroplets using localized electric fields in microfluidic channels, *Langmuir*, 2010, 26, 14443–14449.
- 32 K. Ahn, J. Agresti, H. Chong, M. Marquez and D. A. Weitz, Electrocoalescence of drops synchronized by size-dependent flow in microfluidic channels, *Appl. Phys. Lett.*, 2006, 88, 2014–2017.
- 33 A. R. Abate, C.-H. Chen, J. J. Agresti and D. A. Weitz, Beating Poisson encapsulation statistics using close-packed ordering, *Lab Chip*, 2009, 9, 2628–2631.
- 34 Y. Zhang, *et al.*, A programmable microenvironment for cellular studies via microfluidics-generated double emulsions, *Biomaterials*, 2013, 34, 4564–4572.
- 35 W. Senkowski, *et al.*, Three-Dimensional Cell Culture-Based Screening Identifies the Anthelmintic Drug Nitazoxanide as a Candidate for Treatment of Colorectal Cancer, *Mol. Cancer Ther.*, 2015, 14, 1504–1516.
- 36 K. Y. Lee and D. J. Mooney, Alginate: properties and biomedical applications, *Prog. Polym. Sci.*, 2012, 37, 106–126.
- 37 J. A. Rowley, G. Madlambayan and D. J. Mooney, Alginate hydrogels as synthetic extracellular matrix materials, *Biomaterials*, 1999, 20, 45–53.

